



HSP90 modulates actin dynamics: Inhibition of HSP90 leads to decreased cell motility and impairs invasion

Aftab Taiyab, Ch. Mohan Rao*

Centre for Cellular and Molecular Biology, Council for Scientific and Industrial Research, Hyderabad 500 007, India

ARTICLE INFO

Article history:

Received 23 July 2010

Received in revised form 17 September 2010

Accepted 21 September 2010

Available online 29 September 2010

Keywords:

Actin dynamics

Cell migration

HSP90

17AAG

Invasion

ABSTRACT

HSP90, a major molecular chaperone, plays an essential role in the maintenance of several signaling molecules. Inhibition of HSP90 by inhibitors such as 17-allylamino-demethoxy-geldanamycin (17AAG) is known to induce apoptosis in various cancer cells by decreasing the activation or expression of pro-survival molecules such as protein kinase B (Akt). While we did not observe either decrease in expression or activation of pro-survival signaling molecules in human breast cancer cells upon inhibiting HSP90 with 17AAG, we did observe a decrease in cell motility of transformed cells, and cell motility and invasion of cancer cells. We found a significant decrease in the number of filopodia and lamellipodia, and in the F-actin bundles upon HSP90 inhibition. Our results show no change in the active forms or total levels of FAK and Pax, or in the activation of Rac-1 and Cdc-42; however increased levels of HSP90, HSP90 α and HSP70 were observed upon HSP90 inhibition. Co-immuno-precipitation of HSP90 reveals interaction of HSP90 with G-actin, which increases upon HSP90 inhibition. FRET results show a significant decrease in interaction between actin monomers, leading to decreased actin polymerization upon HSP90 inhibition. We observed a decrease in the invasion of human breast cancer cells in the matrigel assay upon HSP90 inhibition. Over-expression of α B-crystallin, known to be involved in actin dynamics, did not abrogate the effect of HSP90 inhibition. Our work provides the molecular mechanism by which HSP90 inhibition delays cell migration and should be useful in developing cancer treatment strategies with known anti-cancer drugs such as cisplatin in combination with HSP90 inhibitors.

© 2010 Elsevier B.V. All rights reserved.

1. Introduction

The heat shock protein 90 (HSP90) is an ATPase-directed molecular chaperone, which comprises 1–2% of the total cellular protein content [1]. Its contribution to various cellular processes including signal transduction, protein degradation, protein folding, maturation of client proteins [2] and protein trafficking among sub-cellular compartments has been extensively studied [1,3,4]. HSP90 is up-regulated in cancer and its ATPase activity is increased ~50-fold [2], marking it as a promising target for anti-cancer therapy. The cell permeable HSP90 antagonist 17-allylamino-demethoxy-geldanamycin (17AAG) [5–7], presently in phase III clinical trials, competes with ATP and inhibits the ATPase activity of HSP90 [7]. Studies from our laboratory and others have shown that inhibition of HSP90 by geldanamycin and 17AAG leads to induction of apoptosis in various tumor cell types including solid tumors [8,9]. Metastasis, cancer cell migration and invasion into adjacent tissues and intravasation into blood/lymphatic vessels [10], is the cause of most cancer deaths [11]. Thus, a combined strategy of

eliminating the cancer cells by inducing apoptosis and preventing metastasis should be more effective in treatment of cancer.

Cell migration during different processes such as differentiation and cancer is regulated by different mechanisms [12] which are common to both neoplastic and cancer cells. Cell migration requires extensive reorganization of actin network involving equilibrium processes (actin dynamics) between its globular (G) and filamentous (F) forms [13]. Reorganization of actin in response to environmental stimuli, such as extra-cellular matrix (ECM) molecules (e.g. fibronectin) and growth factors, leads to formation of cell protrusions, lamellipodia and filopodia which act as locomotory and sensory apparatus of the cell help in its guided motion [14]. Cancer cells also use these protrusions for migration through the ECM to establish new tumor sites [13]. Rho small family GTPases such as Rho, Rac and Cdc42 [15] play a role in regulating the cytoskeleton by binding GTP and recruiting a range of target proteins thereby bringing about actin reorganization. Rho A promotes formation of actin stress fibers and leads to generation of contractile forces [16,17]. Rac1 signaling promotes formation of large membrane protrusions (branched network of actin) called lamellipodia [18], whereas Cdc42 signaling leads to the formation of actin-rich spikes called filopodia [15]. These proteins are known to activate the actin-related protein (Arp) 2/3 complex, resulting in rapid actin polymerization at sites where rearrangements of actin cytoskeleton is needed [19,20]. Inhibition

* Corresponding author. Centre for Cellular and Molecular Biology, Uppal Road, Hyderabad 500 007, India. Tel.: +91 40 27192543; fax: +91 40 27160591.

E-mail address: mohan@ccmb.res.in (C.M. Rao).

of these protrusions/processes impairs cell migration and hence metastasis.

HSP90 is known to bind actin *in vitro* [20–22]; however its function with respect to actin dynamics is unclear. Proteomic analysis of tumor cell pseudopodial protrusions showed higher levels of HSP90 compared to the cell body [23]. HSP90 is important in maintaining cell morphology, migration and activation of matrix metalloproteinase 2 (MMP2), a key player in matrix degradation and cancer cell invasion [24–26]. However, the higher level of HSP90 observed in tumor cell protrusions and its relation to actin dynamics and cell migration are not well understood.

We have investigated the effect of HSP90 inhibition by 17AAG on the migration, actin dynamics and signaling pathways in transformed rat fibroblast cells, F111, and MDA-MB-231 human breast cancer cells. Our study reveals the mechanistic details involving multiple pathways such as binding to G-actin and inhibiting its polymerization, decreasing RhoA levels and decreasing the translocation of HSP90 α to the cell surface upon HSP90 inhibition.

2. Materials and methods

2.1. Plasmids, drugs and antibodies

The constructs ECFP-Actin and EYFP-Actin were a gift from Dr. Yasunori Hayashi (RIKEN-MIT Neuroscience Research Centre, Massachusetts, USA). The α B-crystallin-FLAG fusion construct was described previously [27].

17-AAG (NIH, Bethesda, Maryland, USA) was dissolved in DMSO (Sigma, USA) and was used at a final concentration of 2 μ M. DMSO-treated cells were considered as control cells.

Primary antibodies FAK (#3258), p-Tyr397-FAK (#3281), paxillin (#2542), p-Tyr118-paxillin (#2541), P-38 (#9212) and p-Thr202/Tyr204-ERK1/2 (#9101) were obtained from Cell Signaling (Beverly, MA, USA). Antibodies for HSP90 (#SPA-846), HSP90 α (#SPS-771), HSP90 β (#SPA-842), HSP70 (#SPA-810), HSP25 (#SPA-801), HSP27 (#SPA-800), α B-crystallin (#SPA-223) and p-Ser-59- α B-crystallin (#SPA-227) were obtained from Stressgen (Victoria, BC, Canada). Antibodies for RhoA (#sc-179), mDia2 (#sc-55540), Cdc42 (#sc-8401), Akt1/2 (#sc-8312) and p-Thr308-Akt1/2 (#sc-16646-R) were obtained from Santa Cruz Biotechnology (Santa Cruz, CA, USA). RhoA (#05-778), Rac1 (#05-389) and Arp2/3 (#07-227) were from Upstate (Lake Placid, NY, USA). GAPDH (#MAB374) and Actin (#MAB1501) were obtained from Chemicon International (Temecula, CA, USA). p-Thr180/Tyr182-P-38 (#612280) was from BD Transduction Laboratories (San Diego, CA, USA). Horse radish peroxidase (HRPO)-conjugated anti mouse/rabbit was obtained from Roche (Indianapolis, IN, USA) and HRPO conjugated anti-goat was obtained from Stressgen (Victoria, BC, Canada). Secondary antibodies for immunofluorescence were obtained from Molecular Probes (Eugene, OR, USA), Zymed Laboratories (San Francisco, CA, USA) and Sigma (St. Louis, USA).

2.2. Cell culture, transfection, and stable clone selection

Transformed rat fibroblast cell line, F111, and human breast cancer cell line, MDA-MB-231 were obtained from American Type Culture Collection (ATCC, USA) and maintained in DMEM (Invitrogen, USA) supplemented with 10% FBS (Invitrogen, USA) in a humidified incubator at 37 °C with 5% CO₂. Cells, when 80% confluent, were transfected with 200 ng of vector using Lipofectamine-2000™-plus reagent (Invitrogen, USA) diluted in incomplete DMEM. Incomplete DMEM was replaced with DMEM supplemented with 10% FBS after 24 h of transfection. The cells treated with or without HSP90 inhibitor were fixed for immunostaining with formaldehyde.

For generation of stable clones, MDA-MB-231 cells after transfection serially diluted against DMEM to 1:1000, 1:500, 1:250 and 1:100 and allowed to grow in the selection medium containing Geneticin

(G418) (800 μ g/ml). Single colonies were picked and plated on 96-well plate. The clones were further passaged (using 24-well plate and then into T-25 flasks). The clones were screened for the protein expression by immuno-blot and immunofluorescence. The positive clones were selected and used for further experiments.

2.3. Immuno-blot analysis and fluorescence microscopy

Whole cellular protein was extracted by incubating cells in 50 mM Tris-Cl buffer, pH-8.0, containing, 1% Triton X-100, 1% sodium deoxycholate, 0.1% sodium dodecyl sulphate, 150 mM sodium chloride, 1 \times protease inhibitor (Sigma), 1 \times phosphatase inhibitor (Sigma) and 1 mM sodium orthovanadate for 30 min on rotator at 4 °C. The mix was centrifuged at 4500 g for 25 min at 4 °C. The protein in the resulting supernatant was quantified by the Bradford method (Biorad, Hercules, CA, USA) according to the instructions of the manufacturer, diluted 1:4 in protein SDS loading buffer, and heated to 95 °C for 5–10 min. A total of 50 μ g of protein was loaded onto 8%, 10% and 12% Tris-HCl SDS-polyacrylamide electrophoresis gels as required, transferred to Hybond C-extra nitrocellulose membrane (Amersham Biosciences, NJ, USA) using wet transfer apparatus (Biorad, Hercules, CA, USA). The membrane was then incubated in blocking solution (5% BSA in Tris Buffered Saline (TBS) containing 0.1% Tween-20) for 2 h with gentle rocking at room temperature. Primary antibody was diluted (in 3% BSA in TBS) according to the prescribed dilutions by the manufacturer or was standardized by checking various dilutions. The membrane was incubated for 3–4 h at room temperature or overnight at 4 °C in primary antibody. After washing for 10 min in TBS containing 0.1% Tween-20 (TBST) thrice, the membranes were incubated in secondary antibody conjugated with HRPO. After washing for 10 min in TBST thrice, the substrate (BM Chemiluminescence kit, Roche) was added on the membrane and was developed using Kodak X-ray films.

For immunofluorescence analysis, cells were fixed in 3.5%–4% formaldehyde with 0.5% Triton X-100 + 0.05% Tween-20/PBS, washed three times with PBS and incubated with rhodamine-phalloidin (1:100; Molecular Probes, Eugene, OR) for 1 h before three washes with PBS and mounting. For cells that were stained with antibodies, the procedure was essentially as mentioned earlier, except that a primary antibody was used in place of phalloidin before incubation with fluorescently-conjugated secondary antibodies, and then was stained with rhodamine-phalloidin. The cells were analyzed and photographed using a Carl Zeiss 510-Meta LSM or Carl Zeiss 510-Meta LSM with multi-photon laser (Chameleon) microscope (Carl Zeiss, GmbH, Germany) or Leica-TCS-SP5 confocal microscope (Leica Microsystems, Germany). The images were further processed using Adobe Photoshop version-7.0.

2.4. Immuno-precipitation and GTPase activation assay

F111 and MDA-MB-231 cells were incubated with modified RIPA lysis buffer (50 mM Tris-Cl pH-7.4, 150 mM NaCl, 1 mM EDTA, and 1 mM PMSF, 1 \times protease inhibitor, 1 mM sodium orthovanadate and 0.01% NP-40) for 5 min and centrifuged at 10,000 g for 25 min at 4 °C. The supernatant was considered as the soluble fraction and the pellet as the in-soluble fraction. Preclearing of the soluble fraction was done by incubation with Protein A sepharose beads (#17-0469-01, Amersham Biosciences, Uppsala, Sweden) for 1 h in a rotator at 4 °C. The lysate was further incubated with anti-HSP90 antibody for 16–20 h in a rotator at 4 °C. Total cell lysate was used for immuno-precipitation of α B-crystallin. Secondary antibodies coupled with magnetic beads (Bangs Laboratories Inc., Fishers, IN, USA) were added to the mix and was incubated for 4 h in a rotator at 4 °C. The magnetic beads were then precipitated using magnetic adapters and heated at 100 °C after addition of sample solubilizing buffer. The samples were resolved using 12% polyacrylamide gel electrophoresis

and were subsequently transferred to the membrane. Immuno-blot was performed for the proteins of interest.

For GTPase activation assay the protocol provided by the manufacturer of the Rac-Cdc42 activation assay kit (#17-441, Millipore Corporation, Temecula, CA, USA) was followed.

2.5. Wound healing assay and analysis

Wounds were made by scraping with a pipette tip in the confluent culture of cells plated in a 4 mm dish. Wound healing was monitored using 20× objective lens of a live cell microscope (Carl Zeiss, GmbH, Germany), having 5% CO₂ supply at 37 °C, in the presence and absence of 17AAG for 20 h in F111 cells, 28 h in MDA-MB-231 cells and 36 h in CryαB-MDA-MB-231 cells. Image was acquired every 3 min and processed as a movie. Analysis of 20 cells was done by clicking on the nucleus of the cell for each frame using Metamorph software and the average speed and standard error were calculated before plotting the bar graph.

2.6. FRET analysis

MDA-MB-231 cells were co-transfected with constructs ECFP-actin and EYFP-actin in a 4-well chambered cover glass. The cells were incubated with or without 17AAG for 24 h, after 3–4 days of transfection. The confocal microscope (Carl Zeiss 510-Meta) was set using cells transfected with either ECFP-actin or EYFP-actin. FRET (Acceptor Photobleaching) was performed using the macro of the LSM software.

2.7. Scanning electron microscopy of the cells plated on matrigel

MDA-MB-231 and CryαB-MDA-MB-231 cells were plated on layer of matrigel (#354234; Bedford, MA; USA) (diluted 1:1 in PBS) and incubated for 2 days in the presence of complete medium for adhesion. The cells were then incubated with or without HSP90 inhibitor for 24 h and then were fixed with 2.5% glutaraldehyde (diluted in 1× PBS) for 2 h at room temperature. After washing three times with PBS the sample was dehydrated by incubating cells for 10 min in 30% acetone followed by 50%, 70%, and 90% acetone (diluted in PBS). The sample was washed three times for 10 min each in 100% acetone and finally with amyl acetate. Critical point drying of the sample was done and scanning electron microscopy (Hitachi, Japan) was performed.

2.8. Analysis of cell migration/invasion assay

F111, MDA-MB-231 and CryαB-MDA-MB-231 cells were plated on the upper chamber of the collagen IV (final concentration-50 µg/µl; #C5533, Sigma, St. Louis, USA) coated 12-well transwell separated with a membrane having 5 µm pore size (#3421, Costar, Corning, NY, USA). The cells were allowed to adhere for 24 h. The cells were then allowed to migrate to the other side of the membrane, with the upper chamber having serum-free DMEM with or without 17AAG and the lower chamber having serum-containing DMEM. After 24 h, the cells were taken out from the other side of the membrane using a cotton swab and were counted after staining with 0.1% Trypan Blue.

For invasion assay, the upper chamber of the transwell was coated with 100 µl of matrigel (diluted 1:1 in PBS) and left to solidify for 30 min at 37 °C. 100 µl of MDA-MB-231-GFP cells (8×10^5 cells/ml) was plated on the other side of the membrane of the matrigel plugged transwell (that is facing towards the lower chamber). The cells were left to adhere for 4 h and then the transwell was placed in a 24-well plate. The lower chamber was filled with serum-free DMEM with or without 17AAG and the upper chamber was filled with serum-containing DMEM with or without Epidermal Growth Factor (400 ng). The cells were allowed to invade for 24 h and live cell confocal microscopy was performed using the 20× lens of multi-photon laser

of Carl Zeiss 510-Meta multi-photon laser scanning confocal microscope. Analysis and 3D reconstruction of the images were done using Imaris software.

3. Results

3.1. Inhibition of HSP90 function decreases cell motility and cellular protrusions

We performed the scratch wound healing assay in the presence or the absence of HSP90 inhibitor, 17AAG, in F111 and MDA-MB-231 cells. Migration was monitored by time lapsed photography with a live cell microscope and data processed as a movie. F111 cells, incubated with the vehicle (DMSO), migrated in a synchronous manner with an average speed of 17×10^{-4} µm/min (graph, Fig. 1A) and were able to heal the wound in 16 h (Movie M1). However, in the presence of 17AAG, F111 cells migrated almost three-fold slower (6×10^{-4} µm/min; graph Fig. 1A) and stopped migrating after 6 h (Movie M2). In contrast, MDA-MB-231 cells showed non-synchronous motion, with some of the cells squeezing out and migrating faster compared to the others; these cells did not heal the wound even after 28 h (Movie M3). The average speed of MDA-MB-231 cells was found to be 5×10^{-4} µm/min (graph Fig. 1B) while that of MDA-MB-231 cells incubated with 17AAG was found to be 3.2×10^{-4} µm/min. Detailed analysis of the movies reveals development of fine filopodia-like structures at the leading edges of the migrating F111 cells (Movie M1), whereas MDA-MB-231 cells show extensive formation of lamellipodia with dark spots at their leading edges in the absence of 17AAG (Movie M3). Interestingly, we observed occasional retraction of the fine protrusions in addition to the decrease in their number in F111 cells (Movie M2), whereas decreased lamellipodia formation and significant reduction in the dark spots at the leading edges in MDA-MB-231 cells was observed upon HSP90 inhibition (Movie M4).

The initial step in cell migration is the reorganization of actin cytoskeleton. We examined whether HSP90 inhibition leads to alterations in actin reorganization by staining the cells in the wound healing assay with phalloidin, which binds to filamentous actin (F-actin) bundles. Staining with phalloidin reveals fine filopodial structures in F111 cells (Fig. 1C). The DIC image as well as the inset of the DIC image shows a significant number of filopodia all over the cells (Fig. 1C). Inhibition of HSP90 in F111 cells leads to a decrease in the number of filopodia (Fig. 1C). Incubation of MDA-MB-231 cells with 17AAG leads to decrease in the tough cortical actin bundles as seen in the upper z-section of the confocal micrograph (Fig. 1D, panel 2) and a significant decrease in the membrane ruffles (enlarged view, Fig. 1D). Further, both the cell types showed a significant decrease in F-actin. Interestingly, actin bundles at the cell periphery showed curved trajectories upon HSP90 inhibition compared to the actin filaments arranged at higher angles to the cell front in control F111 cells (Fig. 1C) and control MDA-MB-231 cells (Fig. 1D).

Taken together, these data suggested that HSP90 inhibition leads to decreased cell motility, decrease in the number of filopodia and lamellipodia, and tough cortical actin bundles.

3.2. Status of signaling molecules involved in adhesion, actin polymerization and actin dynamics, and levels of heat shock proteins and pro-survival signaling molecules upon HSP90 inhibition

Molecular interactions between the cell and the substratum lead to adhesion; molecular assembly and disassembly at the adhesion points, thereby, regulate cell motility. No significant change in the levels of FAK and Pax, the main molecules of the focal adhesion complex, but a minor increase in p-Tyr397-FAK and a decrease in p-Tyr118-Pax were observed in F111 cells upon HSP90 inhibition (Fig. 2A). Levels of Arp2/3, known to be involved in rapid actin polymerization [28], also did not change upon HSP90 inhibition (Fig. 2A). These results indicate no significant change in

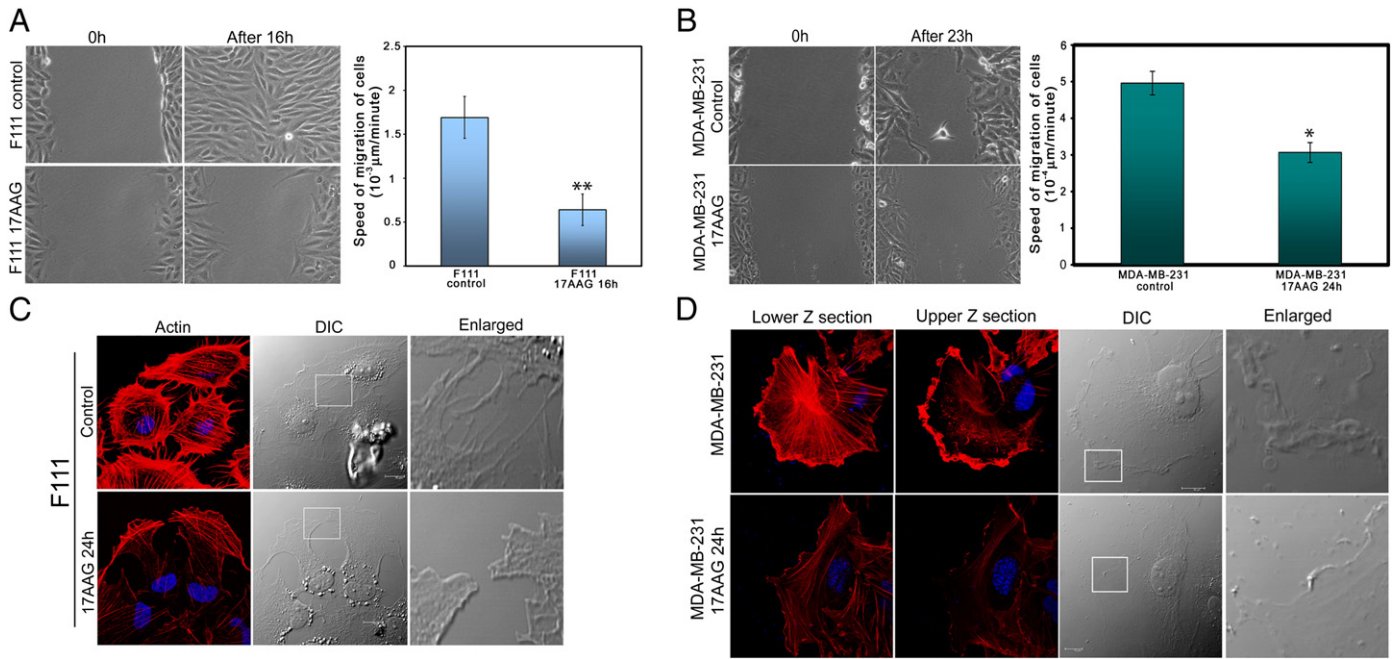


Fig. 1. Decreased motility and cellular protrusions in F111 and MDA-MB-231 cells upon treating with 17AAG for 24 h. (A) Motility of F111 cells in the presence or absence of 17AAG (2 μ M). (B) Motility of MDA-MB-231 cells in the presence or absence of 17AAG (2 μ M). (C) Confocal images of F-actin staining by phalloidin coupled with rhodamine of 17AAG-treated and untreated F111 cells. (D) Confocal images of F-actin staining by phalloidin coupled with rhodamine of 17AAG-treated and untreated MDA-MB-231 cells. The graphs in panels A and C represent the average motility of 20 cells \pm S.E. of two independent experiments. Scale bar in the DIC panel (panels C and D), 10 μ m.

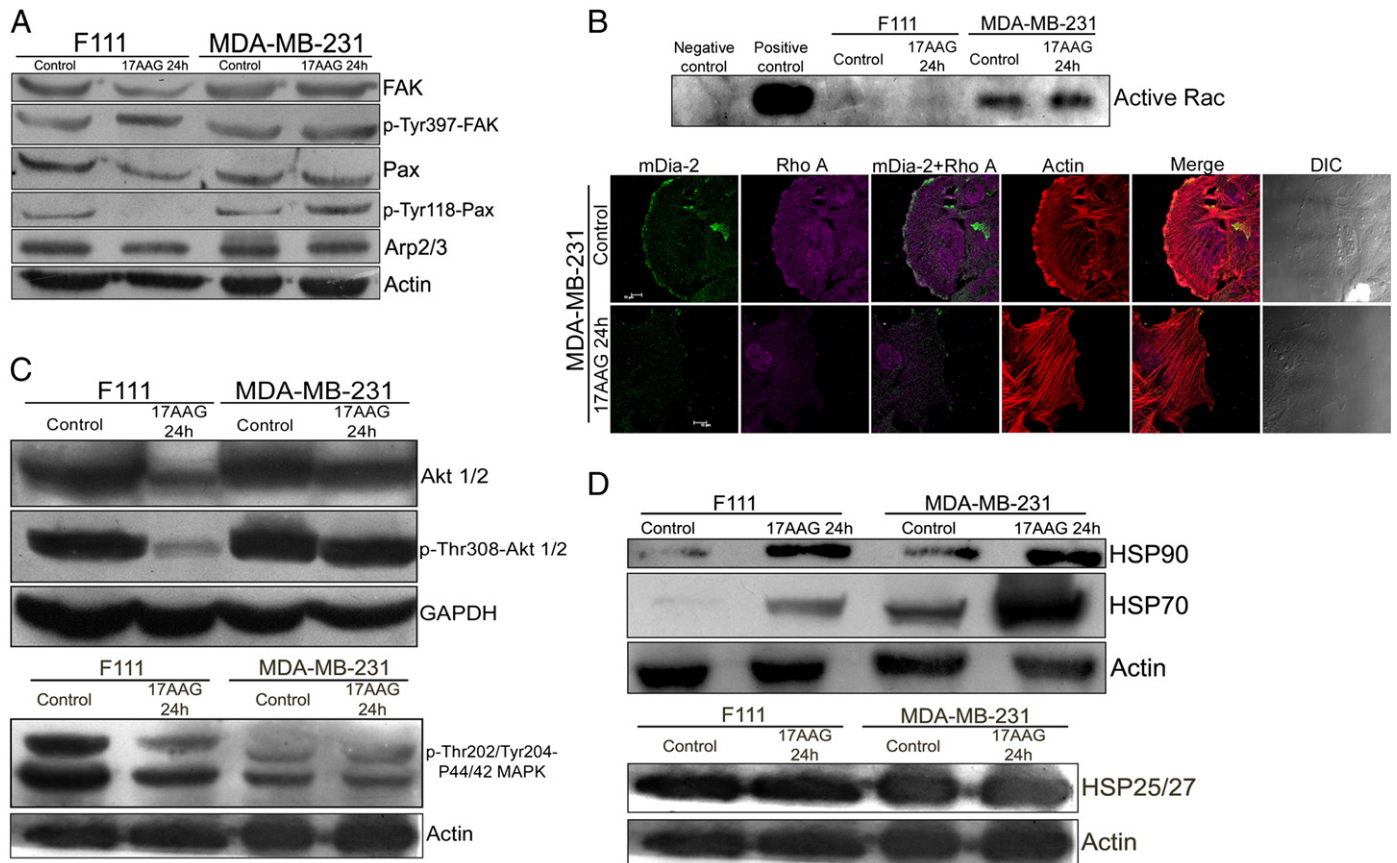


Fig. 2. Change in levels of HSPs and signaling molecules involved in F111 and MDA-MB-231 cells upon HSP90 inhibition. (A) Immuno-blot analysis of FAK, p-Tyr397-FAK, Pax, p-Tyr468-Pax and Arp2/3 in 17AAG-treated and untreated cells. (B) GTPase pull-down for Rac1 (upper panel). Confocal images of RhoA and mDia2 in 17AAG-treated and untreated MDA-MB-231 cells. Scale bar, 10 μ m. (C) Immuno-blot analysis of Akt1/2, p-Ser308-Akt1/2 and p-Thr202/Tyr204-ERK1/2 for 17AAG-treated and untreated cells. (D) Immuno-blot analysis of HSP90, HSP70, HSP25 and HSP27 for 17AAG-treated and untreated cells. Actin is used as a loading control.

the levels of molecules involved in cell adhesion and actin polymerization upon HSP90 inhibition.

We have investigated the status of Rho family of small GTPases, the key regulators of both cell adhesion and actin cytoskeleton, in F111 and MDA-MB-231 cells. No significant change in the levels of Rac1 and Cdc42 (Fig. S1), known to be involved in the formation of lamellipodia and filopodia respectively, was observed upon HSP90 inhibition. Immuno-blot analyses of the GTPase pull-down assay for Rac1 and Cdc42 show no change in the activation of Rac1 (Fig. 2B, upper panel) and Cdc42 (data not shown) upon HSP90 inhibition. We investigated RhoA and mDia2, the proteins known to be involved in the generation of contractile force [16] and in the formation of lamellipodia [29] respectively by immuno-blot and immunofluorescence analysis and found a significant decrease in the level of RhoA and depletion of mDia2 from the cell periphery upon HSP90 inhibition (Figs. 6A and 2B).

Molecules such as Rho GTPases involved in cell migration require phosphorylation by pro-survival signaling molecules [30] such as protein kinase B (Akt) and Extra-cellular Regulated Kinase (ERK). A significant decrease in the levels of Akt1/2 and ERK1/2 was observed in F111 cells upon HSP90 inhibition (Fig. 2C); however, no change in the levels of either inactive or active form of Akt1/2 or active form of ERK1/2 was observed in MDA-MB-231 cells upon incubation with 17AAG (Fig. 2C). Degradation, or decrease in the levels of activation, of these pro-survival signaling molecules due to HSP90 inhibition propels cells to undergo apoptosis [8]. We did not observe apoptosis in either MDA-MB-231 cells or F111 cells until 24 h of HSP90 inhibition.

Up-regulation of HSPs such as HSP70 is known to prevent apoptosis [31]. Immuno-blot analysis shows drastic increase in the levels of HSP90 and inducible form of HSP70, but not in the levels of HSP25/27, upon HSP90 inhibition (Fig. 2D).

3.3. Immuno-precipitation and FRET analysis show interaction of HSP90 with soluble actin

We performed immuno-precipitation of HSP90 from the soluble and the in-soluble fractions of F111 and MDA-MB-231 cell lysates (see Materials and methods) and probed for the proteins involved in cell migration. Immuno-blot analysis of the immuno-precipitated samples shows increase in HSP90 in the soluble fraction upon HSP90 inhibition (Fig. 3A). Interestingly, we observed an increase in the pull-down of actin, possibly G-actin, with HSP90 upon HSP90 inhibition (Fig. 3A) indicating specific interaction of HSP90 with actin in the

soluble fraction. α B-Crystallin also precipitated with HSP90 from the soluble fraction which increased upon HSP90 inhibition in F111 cells (Fig. 3A). We did not observe pull-down of α B-crystallin with HSP90 in MDA-MB-231 cells as these cells express low levels of α B-crystallin (Fig. S2). To confirm the interaction of HSP90 and α B-crystallin, we over-expressed α B-crystallin in MDA-MB-231 cells (Cry α B-MDA-MB-231), performed immuno-precipitation with α B-crystallin and probed for HSP90. We observed pull-down of HSP90 with α B-crystallin in F111 cells and Cry α B-MDA-MB-231 cells (Fig. 3B). Further, we also observed pull-down of α B-crystallin with the immuno-precipitate of HSP90 in MDA-MB-231 cells over-expressing α B-crystallin (Fig. 3A). We also probed for actin in the samples immuno-precipitated for α B-crystallin. These observations clearly suggest increased interaction of HSP90 with soluble form of actin (G-actin) and α B-crystallin upon HSP90 inhibition, which might be responsible for the decreased actin tread-milling at the cell periphery.

To further probe the effect of HSP90 inhibition on actin dynamics, we transfected MDA-MB-231 cells with actin-ECFP and actin-EYFP vector and performed Förster Resonance Energy Transfer (FRET) in the presence and absence of 17AAG. We bleached the acceptor, actin-EYFP, and looked for the increase in the fluorescence of the donor, actin-ECFP. We observed 18% FRET efficiency in control MDA-MB-231 cells (DMSO-treated), whereas MDA-MB-231 cells incubated with 17AAG for 24 h showed ~9% FRET efficiency, a 50% decrease compared to the control cells (Fig. 3C). The decrease in FRET efficiency implies that actin-ECFP and actin-EYFP are unable to interact, thereby leading to blockade of actin tread-milling.

3.4. Inverse invasion assay and scanning electron microscopy reveal decrease in invasion and distortion of morphology of MDA-MB-231 cells

Actin tread-milling and actin cytoskeleton remodeling play an essential role in invasion. We investigated the effect of HSP90 inhibition on invasiveness of MDA-MB-231 cells by inverse invasion assay of MDA-MB-231 cells over-expressing p-EGFP (MDA-MB-231-GFP) in the presence or absence of 17AAG. Confocal micrographs as well as their 3-D reconstruction show that control MDA-MB-231-GFP cells invade the matrigel up to a height of 113 μ m, whereas MDA-MB-231-GFP cells incubated with 17AAG invade up to a height of only 16 μ m (Figs. 4A and S3) indicating decreased invasion of MDA-MB-231-GFP cells upon HSP90 inhibition. Scanning electron microscopic investigation of MDA-MB-231 cells on matrigel (about 500 μ m thick)

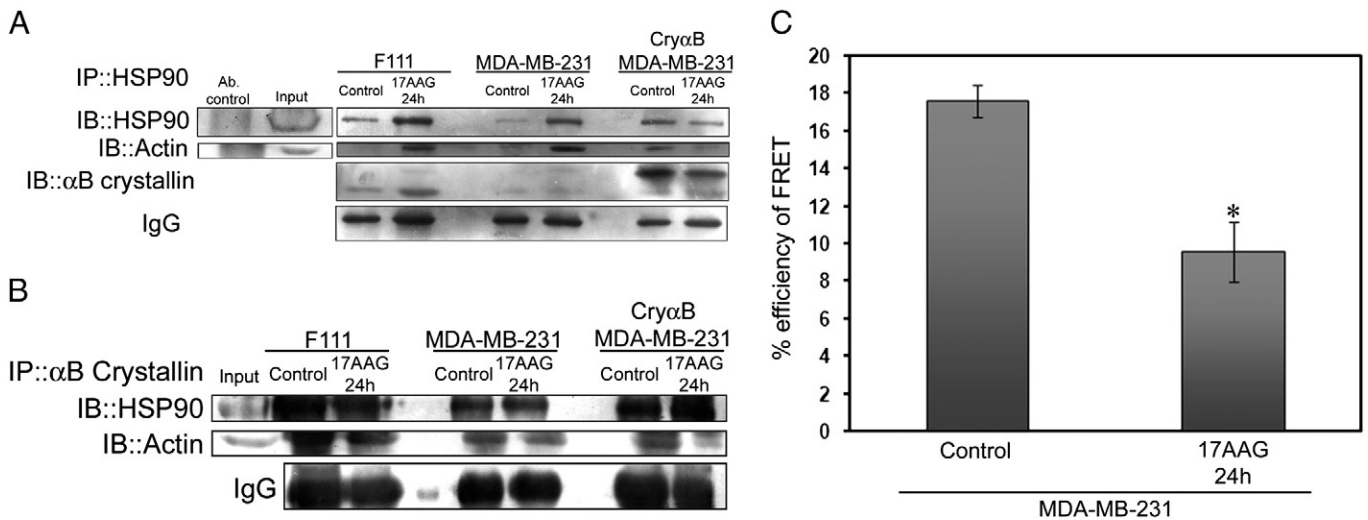


Fig. 3. Increased association of HSP90 with soluble actin and decrease in G-actin interaction upon HSP90 inhibition by 17AAG. (A) Immuno-blot analysis of HSP90 immuno-precipitate probed by actin and α B-crystallin antibodies in the soluble fraction. (B) Immuno-blot analysis of α B-crystallin immuno-precipitate from total cell lysate probed by actin and HSP90 antibodies. (C) FRET analysis of MDA-MB-231 cells co-transfected with actin-ECFP and actin-EYFP constructs. The graph represents the average FRET occurring with and without HSP90 inhibition. Error bars indicate \pm SEM of 12 cells from four independent experiments. *P-value ($p < 0.05$) is in comparison to control.

revealed proper adhesion, spreading and invasion of these cells (Fig. 4B), whereas MDA-MB-231 cells incubated with 17AAG showed severe distortion, shrinkage and detachment from the matrigel (Fig. 4B), thereby leading to a decrease in invasion.

Invasion of cells in the matrigel requires digestion of the matrix. MMP2, MMP9 and MMP14 have been shown to be predominantly involved in degradation of the matrix in tumors [32]. Extra-cellular or surface HSP90 α has been shown to be responsible for the activation of MMP2 [24]. We observed a drastic decrease in surface HSP90 α upon HSP90 inhibition as shown by the large field (20 \times) confocal micrograph (Fig. 4C). We also observed a significant decrease in the number of the cells expressing surface HSP90 α (Fig. 4D) upon HSP90 inhibition.

3.5. Over-expression of α B-crystallin in MDA-MB-231 cells does not abrogate the effect of HSP90 inhibition

α B-Crystallin seems to have a role in breast cancer and its over-expression is proposed to predict poor clinical outcome in breast cancer [33]. Since MDA-MB-231 cells express low levels of α B-crystallin (Fig. S2), we over-expressed α B-crystallin in these cells (Cry α B-MDA-MB-231) and investigated the outcome of HSP90 inhibition. Cry α B-MDA-MB-231 cells appeared to be narrower and resembled epithelial cells more closely compared to MDA-MB-231 cells (unpublished observation). No significant change was observed

in the motility of MDA-MB-231 cells over-expressing α B-crystallin upon HSP90 inhibition (Movies M5 and M6). Staining 17AAG-treated Cry α B-MDA-MB-231 cells for F-actin reveals decreased number of lamellipodia and decrease in tough cortical actin bundles (Fig. 5B).

Earlier reports suggest phosphorylation-dependent (serine-59) localization of α B-crystallin in lamellipodia in porcine lens epithelial cells [34], and association of α B-crystallin with F-actin under stress conditions in cardiomyocytes [35]. While α B-crystallin showed a diffused pattern of staining in control Cry α B-MDA-MB-231 cells and in 17AAG-treated Cry α B-MDA-MB-231 cells, 17AAG-treated cells showed decreased localization of α B-crystallin at the edges of the cell and a significant decrease in the number of lamellipodia (Fig. 5A and B). Immuno-blot analysis revealed increase in α B-crystallin in F111 cells and a minor increase in α B-crystallin in Cry α B-MDA-MB-231 cells accompanied by an increase in the Serine-59-phosphorylation of α B-crystallin in F111 and Cry α B-MDA-MB-231 cells upon HSP90 inhibition (Fig. 5C). p38 MAP kinase is known to phosphorylate α B-crystallin at Ser-59 residue [36]. Immuno-blot analysis of phospho-p38 MAP kinase revealed no activation of p38 MAP kinase in either MDA-MB-231 or Cry α B-MDA-MB-231 cells (Fig. 5C). On the other hand, both control and 17AAG-treated F111 cells showed comparable activation of p38 MAP kinase (Fig. 5C). In contrast to the previous report [34], we observed decreased localization of phospho-Ser-59- α B-crystallin to the lamellipodia in Cry α B-MDA-MB-231 cells upon HSP90 inhibition (unpublished

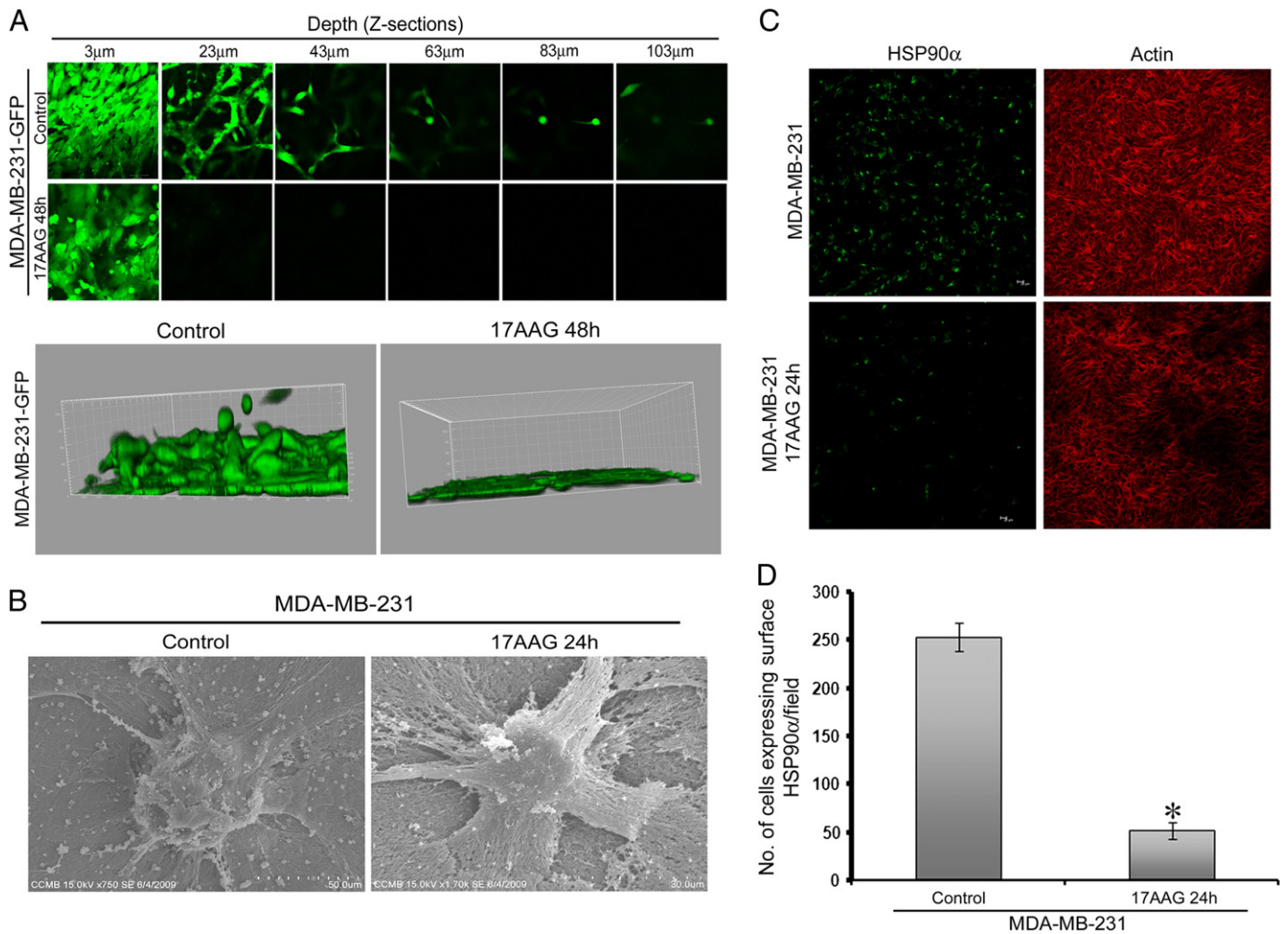


Fig. 4. Inhibition of HSP90 decreases invasion and surface expression of HSP90 α in breast cancer cells. (A) Upper panel shows confocal images of inverse invasion assay for 17AAG-treated and untreated MDA-MB-231-GFP cells. Lower panel shows the 3D reconstruction of the confocal images of inverse invasion assay. Scale bar, 50 μ m. (B) Scanning electron micrographs of control and 17AAG-treated MDA-MB-231 cells plated on matrigel. (C) Immunofluorescence images of surface HSP90 α for 17AAG-treated and untreated MDA-MB-231 cells. Scale bar, 20 μ m. (D) The graph represents the average number of cells expressing surface HSP90 α per field from 4 different fields. Error bars indicate \pm SEM of 4 different fields from 3 independent experiments. *P-value ($p < 0.02$) is in comparison to control.

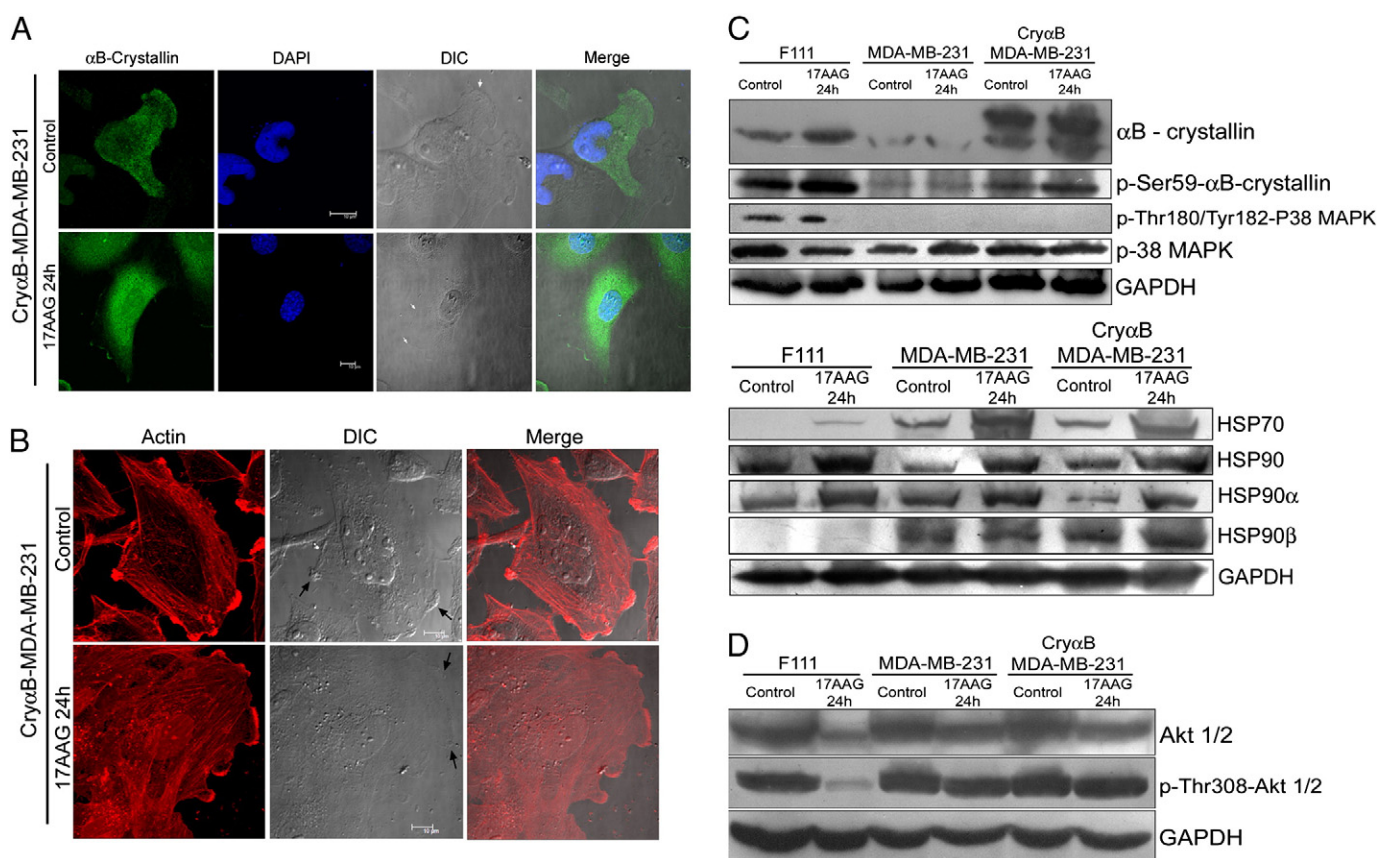


Fig. 5. Localization and expression of α B-crystallin and actin, and expression levels of heat shock proteins and pro-survival signaling molecules in Cry α B-MDA-MB-231 cells upon HSP90 inhibition. (A) Immunofluorescence images of α B-crystallin for 17AAG-treated and untreated Cry α B-MDA-MB-231 cells. Scale bar, 10 μ m. (B) Rhodamine-phalloidin staining for actin in 17AAG-treated and untreated Cry α B-MDA-MB-231 cells. Scale bar, 10 μ m (C) Immunoblot analysis of α B-crystallin, p-Ser59- α B-crystallin, p-Thr180/Tyr182-P38 MAP kinase, P-38 MAP kinase (upper panel) and of HSP90, HSP90 α , HSP90 β and HSP70 (lower panel) of 17-AAG treated and untreated F111, MDA-MB-231 and Cry α B-MDA-MB-231 cells. (D) Immunoblot analysis for Akt1/2 and p-Thr308-Akt1/2 expression in 17AAG-treated and untreated F111, MDA-MB-231 and Cry α B-MDA-MB-231 cells. GAPDH was used as a loading control.

observation) despite the increase in the protein levels of phospho-Ser-59- α B-crystallin (Fig. 5C).

We have investigated whether over-expression of α B-crystallin leads to any alteration in the expression of other heat shock proteins. Upon HSP90 inhibition, we observed a significant increase in the levels of HSP70, HSP90 and HSP90 α , but not in HSP90 β in Cry α B-MDA-MB-231 cells (Fig. 5C). Further we did not observe any change in the levels of Akt and p-Thr308-Akt in Cry α B-MDA-MB-231 cells upon HSP90 inhibition (Fig. 5D). Our data shows that Cry α B-MDA-MB-231 cells show similar cell motility profile, pattern of actin distribution, and profile of different HSPs as shown by MDA-MB-231 cells upon HSP90 inhibition.

3.6. Expression of signaling molecules involved in cell adhesion, survival and transwell migration assay and scanning electron microscopic study of Cry α B-MDA-MB-231 cells

Because we observed no significant change in the motility of MDA-MB-231 cells over-expressing α B-crystallin upon HSP90 inhibition, we assessed the profile of signaling molecules involved in cell proliferation and adhesion. No change in the levels of Rac1 and Cdc42 (Fig. S1) as well as RhoA (Fig. 6A) was observed in Cry α B-MDA-MB-231 cells upon HSP90 inhibition. In contrast MDA-MB-231 cells show a significant decrease in the levels of RhoA, upon HSP90 inhibition, as shown by immuno-blot and immuno-staining experiments. We observed no change in the levels of active or inactive Akt1/2 in both MDA-MB-231 and Cry α B-MDA-MB-231 cells upon HSP90 inhibition (Fig. 6B).

In order to investigate any alteration in migration of Cry α B-MDA-MB-231 cells upon HSP90 inhibition we performed transwell migration assay. Though the percentage of F111, MDA-MB-231 and Cry α B-MDA-MB-231 cells which migrated to the other side of the membrane of the transwell decreased upon HSP90 inhibition, we observed a minor but significant increase in the migration of Cry α B-MDA-MB-231 cells compared to that of MDA-MB-231 cells (Fig. 6C). Scanning electron micrographs of Cry α B-MDA-MB-231 cells plated on matrigel showed that the cells adhered to the matrigel with some cells migrating inside the matrigel. 17AAG-treated Cry α B-MDA-MB-231 cells showed severe distortion in the cell morphology and rupture in the connection of Cry α B-MDA-MB-231 cells with the matrigel in addition to impairment in cell adhesion (Fig. 6B). Together, these data suggest that over-expression of α B-crystallin in MDA-MB-231 cells does not lead to any observable change in the property of cell migration and invasion upon HSP90 inhibition.

4. Discussion

HSP90 inhibition has been known to induce apoptosis in cancer cells [8,9]. We did not observe apoptosis in 17AAG-treated F111 or MDA-MB-231 cells. The reason could be the observed increase in levels of HSP70, HSP90 and α B-crystallin, which are known to protect cells from heat-induced apoptosis [31]. However, importantly our study shows that 17AAG acts as an antagonist to cancer cell motility, migration and invasion. Increase in the level of α B-crystallin but not that of HSP25 reveals differential activation of small heat shock

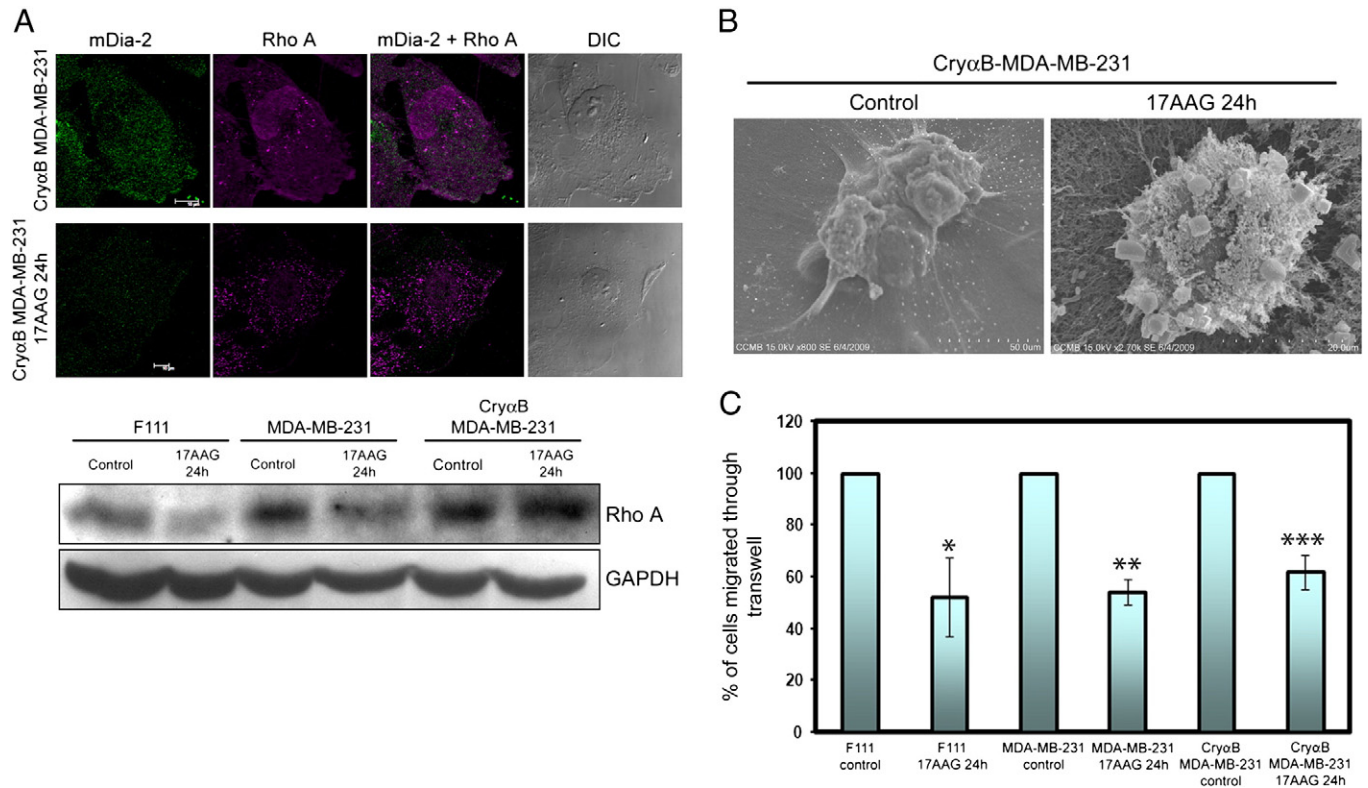


Fig. 6. Expression and localization of signaling molecules, transwell migration assay and matrigel studies for Cryo α B-MDA-MB-231 cells. (A) 17AAG-treated and untreated Cryo α B-MDA-MB-231 cells were stained for RhoA and mDia2 (upper panel). Scale bar, 10 μ m. Lower panel shows the immuno-blot of RhoA for 17AAG-treated and untreated F111, MDA-MB-231 and Cryo α B-MDA-MB-231 cells. (B) Scanning electron micrographs of control and 17AAG-treated Cryo α B-MDA-MB-231 cells plated on matrigel. (C) Transwell migration assay for 17AAG-treated and untreated F111, MDA-MB-231 and Cryo α B-MDA-MB-231 cells. The graph represents the average percentage normalized with the respective controls. Error bars indicate \pm SEM of three independent experiments done in triplicate.

proteins upon HSP90 inhibition, the molecular basis of which is not clear.

Lamellipodia and filopodia are the essential locomotory and sensory apparatus of the cell. HSP90 inhibition leads to significant reduction in the number of filopodia and retraction of filopodial protrusions in F111 cells (Fig. 1C). Incubation of MDA-MB-231 cells with 17AAG leads to a significant decrease in lamellipodia, tough cortical actin bundles (see Movie M3) as well as membrane ruffles (Fig. 1D). The cellular protrusions are predominantly composed of array of actin bundles arranged parallelly in filopodia and trajectorially in lamellipodia. Koestler et al. [37] have shown that the curved arrangement of F-actin bundles at the leading edges during cell migration leads to pausing and retraction of the cell. Our analysis of the F-actin-stained cells shows arrangement of F-actin parallel to the cell membrane of the migrating cells indicating pause, and not retraction, in cell motility. Dynamic equilibrium between G-actin and F-actin, predominantly at the lagging and leading edges of the migrating cell is important for the formation of cellular protrusions. We observed no change in the levels of total actin but a decrease in F-actin upon Hsp90 inhibition, suggesting a shift in the equilibrium from F- to G-actin. The level of Arp2/3 does not change upon HSP90 inhibition, suggesting that molecules involved in actin polymerization are not responsible for HSP90 inhibition-mediated decrease in F-actin.

HSP90 inhibition led to a decrease in the efficiency of FRET between actin molecules. We hypothesize that HSP90 interacts with and sequesters G-actin, and hence does not allow the polymerization of G-actin monomers. In fact, co-immuno-precipitation experiments show interaction of HSP90 with G-actin. HSP90 inhibition leads to, *inter alia*, increase in the level of HSP90 which sequesters more G-actin, shifting the polymerization-depolymerization equilibrium predominantly at the leading edge of the migrating cells. This process might contribute to the observed decrease in numbers of filopodia and lamellipodia upon

HSP90 inhibition (Fig. 3A and C). Interaction of HSP90 with its client proteins is an ATP-dependent process which gets disrupted due to HSP90 inhibition by 17AAG [3,5]. In contrast, interaction of HSP90 with G-actin seems to be ATP-independent as we observed an increase rather than a decrease in the interaction of HSP90 with G-actin. The increased interaction of HSP90 with G-actin can be co-related with the increase in the levels of HSP90, upon HSP90 inhibition by 17AAG, which is due to the increase in the activity of heat shock transcription factor 1 (HSF1) (unpublished observation). The decrease in the levels of RhoA upon HSP90 inhibition suggests a decrease in the generation of contractile forces necessary for cell motility.

Though HSP90-dependent phosphorylation of focal adhesion kinase (FAK) is shown to be important in VEGFR2-mediated cell migration [38], we did not observe change in the levels of phosphorylated or unphosphorylated forms of FAK in MDA-MB-231 cells. We found that though the total level of paxillin, a focal adhesion-associated adaptor protein, did not change, the level of its active form decreased in F111 cells upon HSP90 inhibition.

Actin dynamics-mediated cellular protrusion is responsible for cell migration and invasion of matrix, the primary step in cancer cell metastasis. MDA-MB-231 cells underwent severe distortion of morphology (Fig. 4B), had decreased lamellipodia and showed decreased matrigel invasion upon HSP90 inhibition (Fig. 4A) establishing a correlation between actin dynamics, formation of cellular appendages and cell invasion in the context of HSP90 and its inhibition. Extra-cellular HSP90 plays an important role in immune response, invasion and metastasis by its interaction with several extra-cellular clients such as dengue virus receptor, ErbB2 etc [39]. Further, extra-cellular HSP90 α has an important role in the activation of MMP2 [24], degradation of the extra-cellular matrix and invasion; cell-impermeant inhibitors of HSP90 such as DMAG-N-oxide inhibit HSP90 α -mediated invasion of melanoma cells [26]. Our results suggest a decrease in the surface localization of

HSP90 α in MDA-MB-231 cells in spite of the increase in the expression of HSP90 α upon HSP90 inhibition. It is possible that interaction of 17AAG with HSP90 α might decrease its translocation from the cytoplasm to the cell surface.

Moyano et al., have shown that over-expression of α B-crystallin in transformed human mammary epithelial cells leads to increased cell migration and luminal filling in 3D basement membrane cultures compared to normal human mammary epithelial cells. Since we observed a marginal increase in α B-crystallin expression upon HSP90 inhibition in F111 cells, we investigated whether over-expression of α B-crystallin could counter the effect of HSP90 inhibition in MDA-MB-231 cells. Overall, over-expression of α B-crystallin did not significantly alter the effect of HSP90 inhibition on MDA-MB-231 cells.

Taken together, our present findings illustrate the mechanisms underlying inhibition of cell migration and invasion upon HSP90 inhibition through multiple pathways such as binding to G-actin and inhibiting its polymerization, decreasing RhoA levels and decreasing the translocation of HSP90 α to the cell surface. Over-expression of α B-crystallin was not able to rescue the effect of HSP90 inhibition. Our study is useful in understanding the functional role of HSP90 in maintaining cellular homeostasis and as a proof of principle of the clinical usefulness of 17AAG against cancer.

Supplementary materials related to this article can be found online at doi:10.1016/j.bbamcr.2010.09.012.

Acknowledgements

We thank Yasunori Hayashi for Actin-CYFP and Actin-EYFP constructs, Rangaraj N. for technical assistance in confocal microscopy, Laura Machesky and Michael Olson for helpful discussions in regard with invasion assay and Dr. T. Ramakrishna Murti for his help in modifying the manuscript. AT acknowledges the Senior Research Fellowship of the Council of Scientific and Industrial Research, India (CSIR).

References

- [1] J.C. Young, F.U. Hartl, Polypeptide release by Hsp90 involves ATP hydrolysis and is enhanced by the co-chaperone p23, *EMBO J.* 19 (2000) 5930–5940.
- [2] A. Kamal, L. Thao, J. Sensintaffar, L. Zhang, M.F. Boehm, L.C. Fritz, F.J. Burrows, A high-affinity conformation of Hsp90 confers tumour selectivity on Hsp90 inhibitors, *Nature* 425 (2003) 407–410.
- [3] L. Neckers, K. Neckers, Heat-shock protein 90 inhibitors as novel cancer chemotherapeutic agents, *Expert Opin. Emerg. Drugs* 7 (2002) 277–288.
- [4] F. Burrows, H. Zhang, A. Kamal, Hsp90 activation and cell cycle regulation, *Cell Cycle* 3 (2004) 1530–1536.
- [5] L. Neckers, T.W. Schulte, E. Mimnaugh, Geldanamycin as a potential anti-cancer agent: its molecular target and biochemical activity, *Invest. New Drugs* 17 (1999) 361–373.
- [6] T.W. Schulte, L.M. Neckers, The benzoquinone ansamycin 17-allylamino-17-demethoxygeldanamycin binds to HSP90 and shares important biologic activities with geldanamycin, *Cancer Chemother. Pharmacol.* 42 (1998) 273–279.
- [7] C.E. Stebbins, A.A. Russo, C. Schneider, N. Rosen, F.U. Hartl, N.P. Pavletich, Crystal structure of an Hsp90-geldanamycin complex: targeting of a protein chaperone by an antitumor agent, *Cell* 89 (1997) 239–250.
- [8] G.V. Georgakis, Y. Li, G.Z. Rassidakis, H. Martinez-Valdez, L.J. Medeiros, A. Younes, Inhibition of heat shock protein 90 function by 17-allylamino-17-demethoxygeldanamycin in Hodgkin's lymphoma cells down-regulates Akt kinase, dephosphorylates extracellular signal-regulated kinase, and induces cell cycle arrest and cell death, *Clin. Cancer Res.* 12 (2006) 584–590.
- [9] A. Taiyab, A.S. Sreedhar, Ch.M. Rao, HSP90 inhibitors, GA and 17AAG, lead to ER stress-induced apoptosis in rat histiocytoma, *Biochem. Pharmacol.* 78 (2009) 142–152.
- [10] P. Freidl, K. Wolf, Tumor-cell invasion and migration: diversity and escape mechanism, *Nat. Rev. Cancer* 3 (2003) 362–374.
- [11] I.J. Fidler, Selection of successive tumor lines for metastasis, *Cancer Chemother. Pharmacol.* 43 (1999) S3–S10.
- [12] J. Yang, R.A. Weinberg, Epithelial–mesenchymal transitions: at the cross-roads of development and tumor metastasis, *Dev. Cell* 14 (2008) 818–829.
- [13] T.D. Pollard, G.G. Borisy, Cellular motility driven by assembly and disassembly of actin filaments, *Cell* 112 (2003) 453–465.
- [14] H. Yamaguchi, J. Wyckoff, J. Condeelis, Cell migration in tumors, *Curr. Opin. Cell Biol.* 17 (2005) 559–564.
- [15] A.J. Ridley, Rho GTPases and cell migration, *J. Cell Sci.* 114 (2001) 2713–2722.
- [16] M. Amano, Formation of actin stress fibers and focal adhesions enhanced by Rho-kinases, *Science* 273 (1997) 1308–1311.
- [17] K. Kimura, Regulation of myosin phosphatase by Rho and Rho-associated kinase (Rho-kinase), *Science* 273 (1996) 245–248.
- [18] A.J. Ridley, H.F. Paterson, C.L. Johnston, D. Diekmann, A. Hall, The small GTP-binding protein Rac regulates growth factor-induced membrane ruffling, *Cell* 70 (1992) 401–410.
- [19] L.M. Machesky, R.D. Mullins, H.N. Higgins, D.A. Kaiser, L. Blanchoin, R.C. May, M.E. Hall, T.D. Pollard, Scar, a WASP-related protein, activates nucleation of actin filaments by the Arp2/3 complex, *Proc. Natl. Acad. Sci. U. S. A.* 96 (1999) 3739–3744.
- [20] R. Rohtagi, L. Ma, H. Miki, M. Lopez, T. Kirchhausen, T. Takenawa, M.W. Kirschner, The interaction between N-WASP and the Arp2/3 complex links Cdc42-dependent signals to actin assembly, *Cell* 97 (1999) 221–231.
- [21] S. Koyasu, E. Nishida, T. Kodawaki, F. Matsuzaki, K. Iida, F. Harada, M. Kasuga, H. Sakai, I. Yahara, Two mammalian heat shock proteins, HSP90 and HSP100, are actin-binding proteins, *Proc. Natl. Acad. Sci. U. S. A.* 83 (1986) 8054–8058.
- [22] E. Nishida, S. Koyasu, H. Sakai, I. Yahara, Calmodulin-regulated binding of the 90-kDa heat shock protein to actin filaments, *J. Biol. Chem.* 261 (1986) 16033–16036.
- [23] Z. Jia, L. Barbier, H. Stuart, M. Amraei, S. Pelech, J.W. Dennis, P. Metalnikov, P. O'Donnell, I.V. Nabi, Tumor cell pseudopodial protrusions, *J. Biol. Chem.* 280 (2005) 30564–30573.
- [24] B.K. Eustace, T. Sakurai, J.K. Stewart, D. Yimlamai, C. Unger, C. Zehetmeier, B. Lain, C. Torella, W.S. Henning, G. Beste, B.T. Scroggins, L. Neckers, L.L. Ilag, D.G. Jay, Functional proteomic screens reveal an essential extracellular role for HSP90 alpha in cancer cell invasiveness, *Nat. Cell Biol.* 6 (2004) 507–514.
- [25] K. Sidera, M. Samiotaki, E. Yfanti, G. Panayotou, E. Patsavoudi, Involvement of cell surface HSP90 in cell migration reveals a novel role in the developing nervous system, *J. Biol. Chem.* 279 (2004) 45379–45388.
- [26] S. Tsutsumi, B. Scroggins, F. Koga, M.-J. Lee, J. Trepe, S. Felts, C. Carreras, L. Neckers, A small molecule cell-impermeant HSP90 antagonist inhibits tumor cell motility and invasion, *Oncogene* 27 (2008) 1–10.
- [27] A.S. Adhikari, K.S. Rao, N. Rangaraj, V.K. Parnaik, Ch.M. Rao, Heat stress-induced localization of small heat shock protein in mouse myoblast: intranuclear lamin A/C speckles as target for alphaB-crystallin and Hsp25, *Exp. Cell Res.* 299 (2004) 393–403.
- [28] T. Takenawa, H. Miki, WASP and WAVE family proteins: key molecules for rapid rearrangement of cortical actin filaments and cell movement, *J. Cell Sci.* 114 (2001) 1801–1809.
- [29] N. Watanabe, P. Madaule, T. Reid, T. Ishizaki, G. Watanabe, A. Kakizuka, Y. Saito, K. Nakao, B.M. Jockusch, S. Narumiya, P140mDia, a mammalian homolog of *Drosophila* diaphanous, is a target protein of Rho small GTPase and is a ligand for profiling, *EMBO J.* 16 (1997) 3044–3056.
- [30] M. Vicente-Manzanares, D.J. Webb, A.R. Horwitz, Cell migration at a glance, *J. Cell Sci.* 118 (2005) 4917–4919.
- [31] C. Garrido, E. Schmitt, C. Cande, N. Vahsen, A. Parcellier, G. Kroemer, HSP27 and HSP70: potentially oncogenic inhibitors, *Cell Cycle* 2 (2003) 579–584.
- [32] D. Hanahan, R.A. Weinberg, The hallmarks of cancer, *Cell* 100 (2000) 57–70.
- [33] J.V. Moyano, J.R. Evans, F. Chen, M. Lu, M.E. Werner, F. Yehiely, L.K. Diaz, D. Turbin, G. Karaca, E. Wiley, T.O. Nielson, C.M. Perou, V.L. Cryns, α B-Crystallin is a novel oncoprotein that predicts poor clinical outcome in breast cancer, *J. Clin. Invest.* 116 (2006) 261–270.
- [34] R. Maddala, P.V. Rao, α -Crystallin localizes to the leading edges of migrating lens epithelial cells, *Exp. Cell Res.* 305 (2005) 203–215.
- [35] B.N. Singh, K.S. Rao, T. Ramakrishna, N. Rangaraj, Ch.M. Rao, Association of alphaB-crystallin, a small heat shock protein, with actin: role in modulating actin filament dynamics in vivo, *J. Mol. Biol.* 366 (2007) 756–767.
- [36] H. Ito, K. Okamoto, T. Nakayama, K. Isobe, K. Kato, Phosphorylation of alphaB-crystallin in response to various types of stress, *J. Biol. Chem.* 272 (1997) 29934–29941.
- [37] S.A. Koestler, S. Auinger, M. Vinzenz, K. Rottner, J.V. Small, Differentially oriented populations of actin filaments generated in collaborate in pushing and pausing at the cell front, *Nat. Cell Biol.* 10 (2008) 306–313.
- [38] S. Rousseau, F. Houle, H. Kotanides, L. Witte, J. Waltenberger, J. Landry, J. Huot, Vascular endothelial growth factor (VEGF)-driven actin-based motility is mediated by VEGFR2 and requires concerted activation of stress-activated protein kinase 2 (SAPK2/p38) and geldanamycin-sensitive phosphorylation of focal adhesion kinase, *J. Biol. Chem.* 275 (2000) 10661–10672.
- [39] S. Tsutsumi, Len Neckers, Extracellular heat shock protein 90: a role for a molecular chaperone in cell motility and cancer metastasis, *Cancer Sci.* 98 (2007) 1536–1539.